Hidden Neuronal Correlations in Cultured Networks

Ronen Segev, Itay Baruchi, Eyal Hulata, and Eshel Ben-Jacob*

School of Physics and Astronomy, Raymond & Beverly Sackler Faculty of Exact Sciences, Tel-Aviv University, Tel-Aviv 69978, Israel

(Received 14 August 2002; revised manuscript received 29 October 2003; published 19 March 2004)

Utilization of a clustering algorithm on neuronal spatiotemporal correlation matrices recorded during a spontaneous activity of *in vitro* networks revealed the existence of hidden correlations: the sequence of synchronized bursting events (SBEs) is composed of statistically distinguishable subgroups each with its own distinct pattern of interneuron spatiotemporal correlations. These findings hint that each of the SBE subgroups can serve as a template for coding, storage, and retrieval of a specific information.

DOI: 10.1103/PhysRevLett.92.118102 PACS numbers: 87.17.Nn, 05.45.Tp, 84.35.+i

Traditionally, it has been debated whether information stored in time series of neuronal activity is encoded in the temporal locations of firing (time coding) or in the local firing rates (rate coding). It was also proposed that synchrony or correlation between neurons' activities might encode information (see [1,2] for a review). The studies presented here are guided by the assumption that interneuronal correlations do play an important role in information processing. To understand this role, complementary studies of spatiotemporal correlations of recorded activity of *in vivo*, *ex vivo*, and *in vitro* networks are called for [3–8]. The cultured neuronal networks studied here provide relatively simple and well-controlled systems for the *in vitro* investigations. Despite their simplicity, these cultured networks can exhibit rich spontaneous dynamical behavior and also regulate both the morphology of their circuitry and the synaptic strengths to sustain the desired level and structure of their activity [9–18].

The spontaneous activity of isolated networks is studied by growing dissociated cultures of cortical neurons on top of a multielectrode array composed of 60 electrodes. Neurons and glia cells drawn from one-day-old *Charles River* rats are prepared and maintained according to the protocol described in [15]. Subsequently, they are left to spontaneously self-organize within several days into connected and active networks. The networks' activity is noninvasively recorded as several (tens) of the neurons form capacitive coupling with the electrodes, thus enabling the recording of their action potentials. Typical recorded activity is visualized utilizing the raster plot presentation as shown in Fig. 1. Two distinct patterns of activity are transparent: time segments of $\sim$200 ms during which most of the recorded neurons exhibit rapid firing, and long intervals of sporadic neuronal firing separating them. Our goal is to evaluate the correlations between the synchronized bursting events (SBEs) and to relate them with the intra-SBE neuronal activity.

We start with a representation of the nth SBE as a binary matrix located at time T_n within a time window of 400 ms around T_n, which is divided into time bins of 1 ms [19]. For N recorded neurons, the matrix is composed of N rows of 400 bins, each row representing the activity of a specific neuron. The activity of the jth neuron is presented as a binary vector $A^n_{j,l} = 1$, if the jth neuron fired during the lth time bin and zero otherwise. These activity vectors are then convoluted with a normalized Gaussian of width adjusted to the firing rate to obtain a smooth representation of the jth neuron local activity density $D^n_j(t)$ or firing rate, as shown in Fig. 1.

Next, we define $C^{n,m}_i(\tau)$ to be the cross correlation [20,21] between the activity of the ith neuron at the nth SBE and the mth SBE to be

$$C^{n,m}_i(\tau) = D^n_i(t) \otimes D^m_i(t - \tau), \tag{1}$$

where $\otimes$ denotes the standard normalized correlation function between two vectors as a function of the displacement τ. Utilizing these neuronal cross correlations

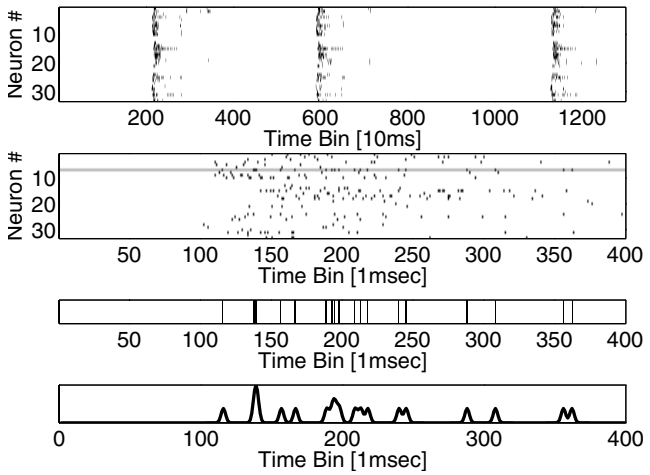

FIG. 1. An example of a raster plot presentation of the recorded network activity showing the synchronized bursting events and a closer look at an individual event (top two boxes). The binary vector of an individual event is shown in the third box and its corresponding activity density $D^n_j(t)$ is shown in the bottom box. A SBE is identified whenever the number of neurons that fired during a time segment of 100 ms exceeds a threshold (usually taken to be 80% of the total number of recorded neurons).

 0031-9007/04/92(11)/118102(4)$22.50

the inter-SBE correlation matrix (or events correlations), $EC(n, m)$, is evaluated by relating

$$EC(n, m) = \max\left(\sum_{i=1}^{N} C_i^{n,m}(\tau)\right), \quad (2)$$

where N is the number of recorded neurons.

A typical example of an inter-SBE correlation matrix for a recorded temporal sequence composed of 300 SBEs is shown in Fig. 2(a). No pronounced organizational motifs or particular patterns can be identified. In order to find out whether such motifs do exist, we use the standard dendrogram clustering method [20,21] for reordering the recorded sequence of SBEs. The idea is to form a new sequence such that highly correlated events will be closely located in the reordered sequence. To do so we utilize the correlation distances $ED(n, m)$ (which represent the distances between the positions of the SBEs in the correlation space) given by

$$ED(n, m) = \left(\sum_{m'=1}^{N_E} [EC(n, m') - EC(m, m')]^2\right)^{1/2}. \quad (3)$$

These distances are used by the dendrogram clustering algorithm to reorder the sequence as we show in Fig. 2(b). The resulting clusterized matrix exhibits a clear block organization, as shown in Fig. 2(c). Such block partitioning indicates that the recorded SBEs sequence is composed of subgroups of distinct SBEs with a mixed temporal order of appearance [22,23].

To further test the general abilities of the method presented here in discovering hidden correlations, we also applied it to recordings from a chemically stimulated (by Ca^{++}) network, described in [24]. The network is first allowed to self-organize at the normal calcium level (0.5 mM) until its spontaneous activity reaches a steady normal level. Then the calcium level is increased to 1 mM. Consequently, the activity becomes more intense for about 20 min, exhibiting wider SBEs and at a higher rate. Afterwards, the network seems to adjust to the new calcium level and the activity becomes similar to the normal one. Long after the 20 min transient time, while the network exhibits normal activity, the calcium level is increased again to 2 mM. In this case the increase in calcium level seems to have a weaker effect on the network activity. We constructed a mixed sequence of 150 SBEs, 50 taken from the normal level of activity at 0.5 mM, 50 from the rapid transient activity at 1 mM, and an additional 50 from the 2 mM. Our dendrogram clustering method exactly identified the three subgroups of SBEs for the three calcium levels with no false positives (see Fig. 3). More important, it was also able to reveal that the 0.5 and 2 mM subgroups have on average higher correlations.

We proceed to relate each subgroup of SBEs with its neuron correlations matrix $NC(i, j)$, defined as

$$NC(i, j) = \sum_{n \epsilon I} D_i^n(t) \otimes D_n^j(t). \quad (4)$$

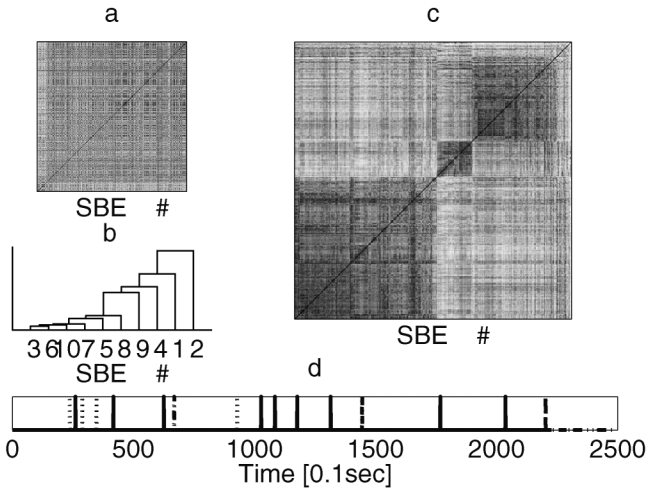

FIG. 2. (a) An example of the inter-SBE correlation matrix $EC(n, m)$ for a sequence of 300 SBEs. The gray levels represent the degrees of correlations using the standard TV scale. (b) A segment of the recorded sequence of the SBEs and their relative distances $ED(n, m)$ represented as the connecting heights. (c) The reordered correlation matrix. Note that this reordered sequence does form a clear block organization hinting about the existence of distinct subgroups of SBEs. (d) A segment of the recorded sequence of SBEs sorted according to the subgroups shown in (c) to demonstrate that they are mixed in their order of temporal appearances.

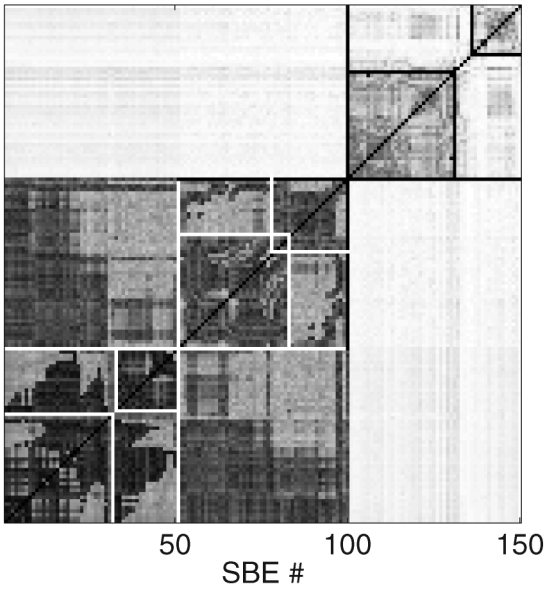

FIG. 3. The correlation matrix for a recorded sequence of SBEs in the presence of different levels of calcium: events No. 1–50, 51–100, and 101–150 correspond to 0.5, 2, and 1 mM extracellular Ca^{++}, respectively.

Note that here the correlation between the ith and the jth neurons at the nth SBE is averaged over the events of the ith subgroup of SBEs. In Fig. 4 we present the neuronal correlation matrix on a corresponding "correlation circle." The neurons are positioned along the circle using the dendrogram algorithm on their correlation distances determined by $ND(i, j)$ [in analogy with $ED(n, m)$]. As is illustrated in Fig. 4 each subgroup of SBEs can be associated with its own specific correlation map on the dendrogram correlation circle.

In brain studies the recorded activity is presented by constructing connectivity networks between the electrode positions according to the evaluated coherence (correlations). Following this approach we also construct similar connectivity networks for our recordings by mapping the neuronal correlations $NC(i, j)$ onto their physical space. That is we link the electrodes according to the computed correlations as is explained and shown in Fig. 4. Comparison between the two formats of presentation reveals interesting features. For example neurons at remote locations in real space, e.g., neurons (24,44) on the top and (24,37) on the bottom can be closely located on the dendrogrammed sequence. The same neuron can assume a very different role at each subgroup of SBEs. For example neuron 25 is highly correlated with many neurons in one subgroup and very weakly correlated in the other.

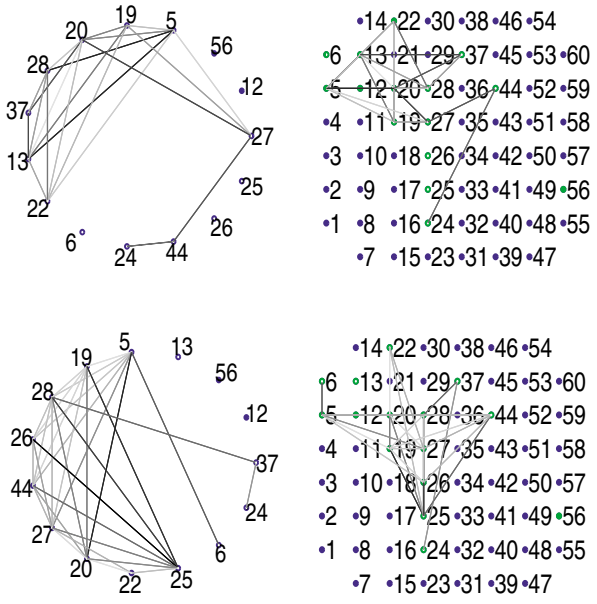

FIG. 4 (color online). The interneuron correlations for the two larger subgroups of SBEs (the larger blocks) shown in Fig. 2(c). On the left we show the dendrogram correlation circle, and on the right the corresponding connectivity networks in the physical space. The links represent the correlations $NC(i, j)$ (using gray levels) above a 0.7 threshold. In this figure the number of each neuron is the number of the electrode through which it is recorded.

Motivated by all of the above, the notion of Synfire chains [25,26] and the observations of "imaginary neurons" [27], we have studied the connections between the temporal partitioning of the SBEs into correlated subgroups and the intra-SBE neuronal activity of each subgroup. Looking for rate ordering, we generated a convoluted raster plot for each block of the inter-SBE correlation matrix. Distinguishable rate ordering patterns are clearly observed, as demonstrated in Fig. 5.

Our findings of temporally mixed distinct subgroups of spatiotemporal correlations, which persist over long times, might hint at the existence of a new neuroinformatic motive. Each kind of SBE can serve as a template to process specific information within its specific neuronal spatiotemporal structure of correlations. This motive can also be tested as a possible new method for storage of information in the *in vitro* networks. The idea is to stimulate a network in parallel at several locations via signals with spatiotemporal correlations similar in structure to those we have recorded. The stimulations should be in bursts separated by time intervals corresponding to the temporal ordering of the measured SBE time series. For

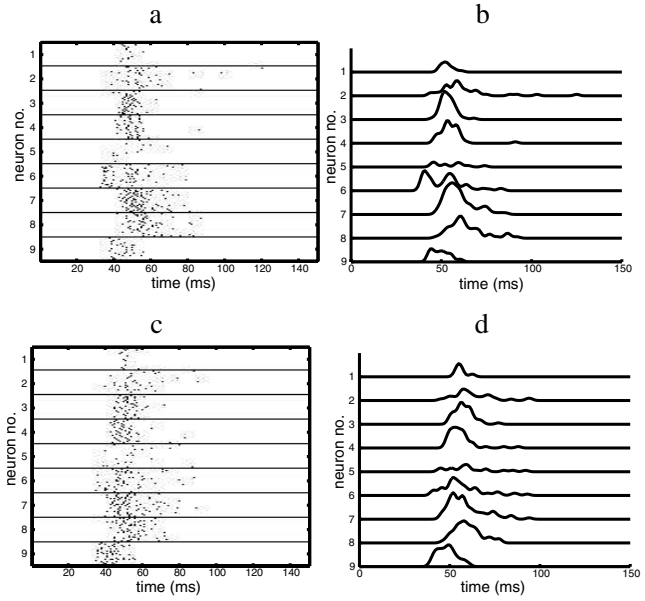

FIG. 5. (a),(c) A raster representation of 20 SBEs simultaneously drawn from the largest subgroups of SBEs (a) and the second largest block (b) (both represented in Fig. 2). Each subgroup of 20 rows represents the firing of a single neuron. The times of the spikes are measured with respect to the SBE time. The neurons fire with a high degree of repetition between successive SBEs. (b),(d). An evaluation of the probability to fire of each neuron during the SBEs from the two larger subgroups. This representation enables one to evaluate the correspondence between the division into subgroups. Note that each neuron has its own delay with respect to the other neurons. For example, the activity of the 6th neuron, which during SBEs from subgroup 1 exhibits three spikes and during subgroup 3 exhibits only one spike.

coding of several messages the network has to be stimulated by a time series composed of temporally mixed bursts, each with its own specific spatiotemporal correlations. Retrieval of the stored information requires a temporal decoding key of the SBEs sequence, which has to be derived from the inverse of the inter-SBE correlation matrix of stimulations. Such studies, although of isolated *in vitro* networks, bear the promise to provide important clues towards solving the long-standing enigma about encoding and retrieval of information both by *in vitro* and also by *in vivo* coupled neuronal networks.

We are very grateful to Professor Sir Sam Edwards and Professor Vipin Srivastava for illuminating conversations especially with respect to function-follow-form relations and the encoding of information. The analyzed data have been recorded during the joint project described in Refs. [15,24]. We are also thankful to Professor Claus-C. Hilgetag for bringing our attention to Refs. [6,8]. We thank I. Brainis for technical assistance in the preparations of the *in vitro* networks. This research has been partially supported by a grant from the Israeli Academy of Sciences, the Sackler Institute, the Adams Super Center for Brain Studies, and the Kodesh Institute.

*Electronic address: eshel@tamar.tau.ac.il

[1] F. Rieke, D. Warland, R. de Ruyter van Stevenink, and W. Bialek, *Spikes: Exploring the Neural Code* (MIT Press, Cambridge, MA, 1997).
[2] W. Gerstner, *Pulsed Neural Networks*, edited by W. Maass and C. B. Bishop (MIT, Cambridge, MA, 1998), pp. 1–51.
[3] B. J. Gluckman, H. Nguyen, S. L. Weinstein, and S. J. Schiff, J. Neurosci. **21**, 590 (2001).
[4] V. L. Towle *et al.*, J. Clin. Neurophys. **16**, 528 (1999).
[5] C-C. Hilgetag, M. A. O'Neill, and M. P. Young, Science **271**, 776 (1996).
[6] K. E. Stephan *et al.*, Philos. Trans. R. Soc. London, Ser. B **355**, 111 (2000).
[7] T. I. Netoff and S. J. Schiff, J. Neurosci. **22**, 7297 (2002).
[8] C. C. Hilgetag, G. A. P. C. Burns, M. A. O'Neill, J. W. Scannell, and M. P. Young, Philos. Trans. R. Soc. London, Ser. B **355**, 91 (2000).
[9] H. P. C. Robinson, M. Kawahara, Y. Jimbo, K. Torimitsu, Y. Kuroda, and A. Kawana, J. Neurophysiol. **70**, 1606 (1993).
[10] R. Segev, Y. Shapira, M. Benveniste, and E. Ben-Jacob, Phys. Rev. E **64**, 011920 (2001).
[11] M. Camepari, M. Bove, E. Maede, M. Cappello, and A. Kawana, Biol. Cybern. **77**, 153 (1997).
[12] S. Marom and G. Shahaf, Q. Rev. Biophys. **35**, 63 (2002).
[13] E. Hulata, R. Segev, Y. Shapira, M. Benveniste, and E. Ben-Jacob, Phys. Rev. Lett. **85**, 4637 (2000).
[14] E. Hulata, R. Segev, and E. Ben-Jacob, J. Neurosci. Methods **117**, 1 (2002).
[15] R. Segev, M. Benveniste, Y. Shapira, E. Hulata, A. Palevski, N. Cohen, E. Kapon, and E. Ben-Jacob, Phys. Rev. Lett. **88**, 118102 (2002).
[16] R. Segev, M. Benveniste, Y. Shapira, and E. Ben-Jacob, Phys. Rev. Lett. **90**, 168101 (2003).
[17] J. M. Beggs, in *Proceedings of the Computational Neuroscience (CNS) Meeting, Chicago, IL, 2002* (Elsevier, Amsterdam, 2002).
[18] J. M. Beggs, and D. Plenz, J. Neurosci. **23**, 11 167 (2003).
[19] To calculate T_n we sum over the neuronal spikes within each bin to calculate its population activity level. Next we convolute the activity with a low pass Gaussian ($\sigma =$ 12.5 ms). The time bin with the maximum population activity marks the location of T_n with an accuracy of ± 10 ms.
[20] Mathworks, http://www.mathworks.com/
[21] W. H. Press, S. A. Teukolsky, W. T. Vetterling, and B. P. Flannery, *Numerical Recipes in C* (Cambridge University Press, Cambridge, UK, 1992).
[22] J. E. Jackson, *A User's Guide to Principal Components* (John Wiley and Sons, Inc., New York, 1991), pp. 1–25.
[23] This notion is justified, provided that the events correlations for SBEs within the same block are substantially higher relative to the events correlations between SBEs from different blocks. Using a χ^2 test [21,22] we find that the corresponding two distributions of correlations are indeed significantly different. Comparisons of the standard deviations of the two distributions yield that the mean correlations within a block and between blocks are 0.81 ± 0.03 ($N = 5551$) and 0.67 ± 0.06 ($N = 9155$), respectively. Note that for artificially generated SBEs (with the same firing rates as that of the recorded data) we obtained 0.69 ± 0.05 ($N = 15753$) and between the artificial SBEs and the recorded ones the values were 0.67 ± 0.07.
[24] R. Segev and E. Ben-Jacob, Physica (Amsterdam) **302A**, 64 (2001).
[25] M. Abeles, *Models of Neural Networks II*, edited by E. Domany, J. L. van Hemmen, and K. Schulten (Springer-Verlag, Berlin, 1994), pp. 121–138.
[26] A Synfire chain is comprised of subgroups of neurons linked by diverging and converging connections. If the connections between the cell in the groups and the size of excitatory postsynaptic potentials are apt, activity can propagate down the chain so that activity in each subgroup of neurons is synchronous (to within about 1 ms) and the subgroups are activated successively to advance the computation being executed.
[27] G. Kreiman, C. Koch, and I. Fried, Nature (London) **408**, 357 (2000).